

GreenEVT: Greensboro Electric Vehicle Testbed

Gustav Nilsson, *Member, IEEE*, Alejandro D. Owen Aquino, *Student Member, IEEE*,
Samuel Coogan, *Senior Member, IEEE*, and Daniel K. Molzahn *Senior Member, IEEE*

Abstract—The ongoing electrification of the transportation fleet will increase the load on the electric power grid. Since both the transportation network and the power grid already experience periods of significant stress, joint analyses of both infrastructures will most likely be necessary to ensure acceptable operation in the future. To enable such analyses, this paper presents an open-source testbed that jointly simulates high-fidelity models of both the electric distribution system and the transportation network. The testbed utilizes two open-source simulators, OpenDSS to simulate the electric distribution system and the microscopic traffic simulator SUMO to simulate the traffic dynamics. Electric vehicle charging links the electric distribution system and the transportation network models at vehicle locations determined using publicly available parcel data. Leveraging high-fidelity synthetic electric distribution system data from the SMART-DS project and transportation system data from OpenStreetMap, this testbed models the city of Greensboro, NC down to the household level. Moreover, the methodology and the supporting scripts released with the testbed allow adaption to other areas where high-fidelity geolocated OpenDSS datasets are available. After describing the components and usage of the testbed, we exemplify applications enabled by the testbed via two scenarios modeling the extreme stresses encountered during evacuations.

Index Terms—electric vehicles, simulator, testbed, power grid, transportation network

I. INTRODUCTION

ELECTRIC vehicles are becoming increasingly popular, with estimates that as much as 15% of the passenger vehicle fleet in the US will be electrified by 2030 [1]. While the electrification of the vehicle fleet brings substantial benefits, such as reduced pollution and noise, electric vehicles (EVs) will also increase the load on the power grid. Most previous research has focused on independently modeling and analyzing either the transportation network or the power grid with, at best, a significantly simplified model of the other infrastructure. The rapid growth in electric vehicles necessitates joint analyses that couple high-fidelity models of electric distribution systems and transportation networks.

High-fidelity simulations can accurately assess the impacts of electric vehicles during normal operations of day-to-day charging and travel [2]–[4]. Moreover, high-fidelity simulations are crucial for modeling extreme events such as evacuations that heavily stress both the transportation network (due to traffic congestion) and the power grid (due to the need for rapid and widespread charging prior to evacuating).

G. Nilsson is with the School of Architecture, Civil and Environmental Engineering, École Polytechnique Fédérale de Lausanne (EPFL), 1015 Lausanne, Switzerland. gustav.nilsson@epfl.ch. A.D. Owen Aquino, D.K. Molzahn, and S. Coogan are with the School of Electrical and Computer Engineering, Georgia Institute of Technology, Atlanta, 30332, USA. {aaquino, molzahn, sam.coogan}@gatech.edu. S. Coogan is also with the School of Civil and Environmental Engineering, Georgia Institute of Technology. This work was supported by the Strategic Energy Institute at Georgia Tech.

Since all the traffic is heading in the same direction during an evacuation, standard macroscopic models for traffic become invalid [5]. Furthermore, previously proposed evacuation planning methods [6], [7] may be inapplicable to systems with high penetrations of electric vehicles. These methods focus on scheduling departure routes and times to mitigate traffic congestion during evacuations. Without considering an electric grid model, the charging schedules needed to support the evacuation may overload the electric distribution infrastructure, potentially interrupting the evacuation’s progress [8]. Moreover, charging station infrastructure may be inadequate to support these evacuations [9], [10].

To enable analyses of both normal conditions and extreme events, this paper presents a testbed for high-fidelity simulations of the charging and movement of electric vehicles within a city. The testbed links together two different simulators, the microscopic traffic simulator SUMO [11] and the power grid simulator OpenDSS [12]. With traffic models of individual vehicles and electric distribution system models down to individual households, these simulators represent more granular levels of detail than what is typically possible to analyze analytically. Hence, we envision that this testbed will serve as a validation platform for tasks such as identifying relevant modeling approximations and assessing control strategies developed using less granular models. Similar testbeds for pure transportation applications have previously been proposed, e.g., [13], [14]. Likewise, synthetic power grid datasets have recently been developed for both transmission systems [15]–[19] and distribution systems [20]. As we will discuss more below, our testbed builds on one such electric distribution test system from the SMART-DS project [20], [21].

Much of the previous research on coupled power and transportation systems considers long-term analyses, especially regarding network expansion planning [22], [23]. Some studies, such as [24], explore the interactions between these two systems in the medium- and short-term time scales with applications in charging management and vehicle routing. Additionally, [25] proposes a method for co-simulation of power grid, traffic, and information networks via data interaction and synchronization between various simulation tools (some of which will be also used in this paper). In-depth reviews of the modeling, interdependence, and applications of these coupled system can be found in [26] and [27].

To the best of our knowledge, none of this existing literature develops an integrated open-source tool for microscopic traffic simulation and high-fidelity electric distribution system simulation of a geographically comprehensive area. The main contribution of this paper is thus the description of a ready-to-use testbed for the detailed simulations of the charging and traffic operations of electric vehicles in a moderate-size urban

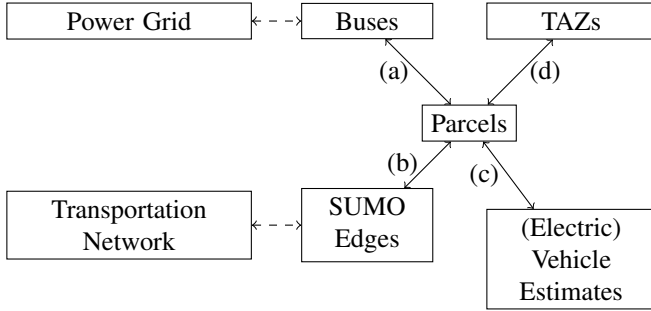


Fig. 1. Conceptual figure of how the different data sources in the testbed are connected. Dashed links represent connections that are already in the respective source data, while the solid links were created through data processing scripts that come with the testbed.

area. We also note that a secondary contribution of this paper is an illustration of how publicly available data from different sources can be combined together to construct testbeds like the one presented in this paper.

The remainder of this paper is organized as follows. In Section II, we describe the role of the testbed’s components and how the data for these components were obtained. In Section III, we give a high-level explanation for how the testbed can be used and the results that can be produced. For a detailed user manual for the testbed, we refer to the documentation available at <https://github.com/GreenEVT/GreenEVT>. In Section IV, we illustrate applications of the testbed via two evacuation scenarios that heavily stress both the power grid and the transportation system.

II. TESTBED COMPONENTS

In this section, we describe the major components of the testbed and their linkages, which are summarized in Figure 1.

A. Power Grid

The key capability of the testbed is the joint simulation of the transportation and electric distribution networks for the city of Greensboro, NC. To accomplish this, the testbed requires granular and high-fidelity electric distribution data for this city. For this purpose, we use one of NREL’s SMART-DS (Synthetic Models for Advanced, Realistic Testing; Distribution systems and Scenarios) datasets [20], [21]. These datasets are large-scale, realistic-but-not-real electric distribution models that capture electrical connections at all levels of distribution systems down to individual households. The datasets are created using information on actual buildings in combination with synthetic loads that have gone through extensive validation to closely match the behavior of real-life distribution systems.

Electric distribution datasets describe components such as generators and loads attached to buses. The buses are connected by lines and transformers to form a network that is typically operated in a radial (tree-like) structure. For the SMART-DS Greensboro dataset used in this testbed, a single bus representing the transmission system is connected to several different substations through subtransmission lines. Then, after each substation, the network is further subdivided into separate components called feeders, which go all the way down to individual consumers. Transformers step down

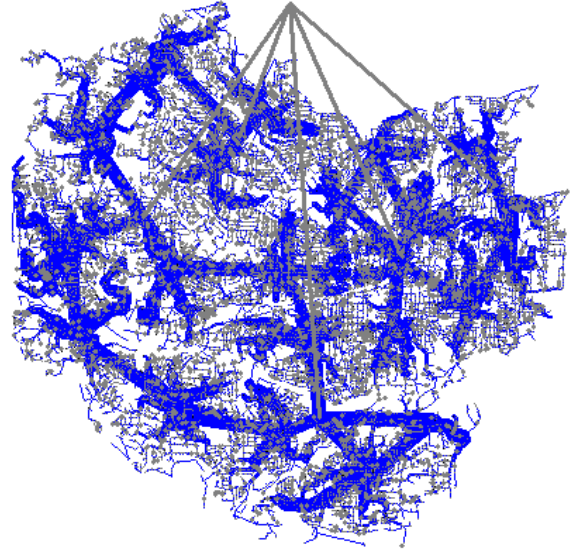


Fig. 2. The urban-suburban distribution network of the SMART-DS Greensboro dataset plotted using OpenDSS.

the voltage at each level of the network. The network is represented by an unbalanced three-phase power flow model which relates the voltages and power injections at each bus and power flows through the lines and transformers.

Each consumer has their own load which we aim to serve without overloading the network’s components. The voltage and current limits of each component as well as the consumer loads are provided by the SMART-DS dataset. Slightly overloading some components for a brief period of time might not result in severe damage but repetitive small overloads contribute to loss-of-life for the components. Large overloads can trigger protection mechanisms to avoid severe damage to components, which could leave large numbers of customers without electric service.

The full SMART-DS Greensboro dataset contains three separate regions, denoted as “industrial”, “rural”, and “urban-suburban”. In this testbed, we simulate the urban-suburban region shown in Figure 2, which contains 21 substations, 61 feeders, 154,241 buses and 218,166 total devices. The dataset also includes both peak planning loads and yearly timeseries loads. For the purposes of the testbed, we focus on the peak planning loads. The total active peak load for the urban-suburban region of Greensboro is 612.7 MW. To model electric vehicle charging, we recursively modify individual loads depending on the electric vehicles’ placements contained in the testbed’s database and vehicle charging schedules informed by the traffic simulations. By default, we assume a constant charging rate of 7.2 kW for each electric vehicle to match the most commonly used EV Level 2 charging equipment [28].

To compile the electric network and run power flow simulations, we use EPRI’s Open Distribution System Simulator, OpenDSS [12].¹ Given a specific load profile, these power flow simulations compute the amount of power and current flowing through each component in the system as well as the voltages at each bus using a Newton-Raphson method. These

¹<https://sourceforge.net/projects/electricdss>

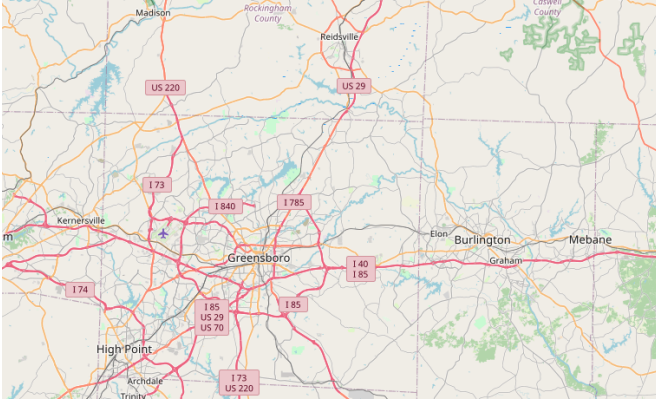


Fig. 3. The area of the transportation network considered. Picture from OpenStreetMap.org.

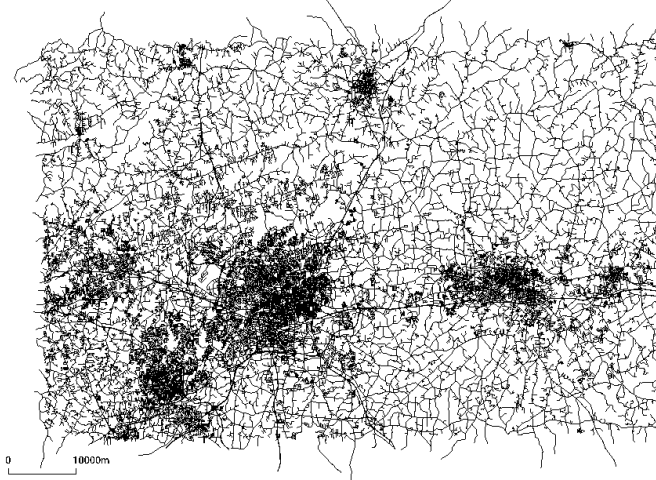


Fig. 4. The road network imported in SUMO.

results thus indicate which components are operating at or beyond their specified limits. Following OpenDSS's default behavior, we allow the simulator to perform transformer tap changes, switch capacitors, and regulate voltages to decrease the number of components operating beyond these limits. By using the COM interface in an external programming language, one can also use the simulator to export network data, modify system components, execute custom time simulations, and print detailed solution reports. The details for each OpenDSS network component, including load models, transformer settings, and voltage bases are defined in the SMART-DS dataset.

To connect the buses in the electric distribution network, whose geographical position is shown in Figure 5, with other components in the testbed, we leverage the geographic coordinates of each bus in the power network dataset to connect each parcel (i.e., an individual plot of land or real estate property) in the area served by the electric distribution system to the closest bus. This is schematically indicated by link (a) in Figure 1.

B. Transportation Network

The transportation network in the testbed was imported from OpenStreetMap using the tool osmWebWizard.² The map

²<https://sumo.dlr.de/docs/Tools/Import/OSM.html>

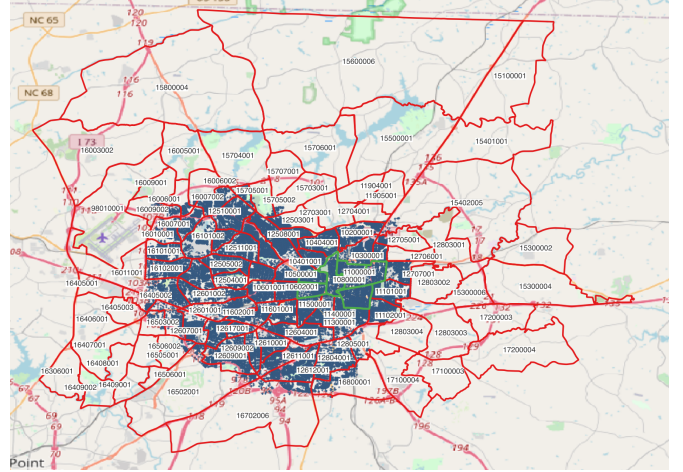


Fig. 5. The TAZs in the area of interest. In total, we have selected 106 TAZs, covering the city center's central area and its surroundings. The colored region contains the buses in the power grid network. The green outlined area denotes the six TAZs we are using in the small evacuation scenario described in Section IV.

TABLE I
PROPERTIES OF THE TRANSPORTATION NETWORK.

Total road length	28216 km
Total lane length	30625 km
No of signalized junctions	914
No of SUMO nodes	50109
No of SUMO edges	118289

covers a rectangular area³ as shown in Figure 3. The imported SUMO network is shown in Figure 4. Table I overviews the transportation network properties, where an edge in SUMO represents a road or a part of a road. Leveraging functions in the SUMO Python Library, Sumolib, we located the closest edge to each parcel and saved the corresponding identifier for the SUMO edge in the testbed's parcel table, i.e., made linkage (b) in Figure 1. Using the number of vehicles associated with each parcel along with this linkage, the testbed inserts the vehicles into the SUMO simulator once a vehicle is scheduled to depart.

C. Parcel Data and Vehicle Estimation

As shown in Figure 1, the parcel data plays a central role in the testbed. Using public data sources about Guilford County, where Greensboro is located, from the state of North Carolina,⁴ the testbed incorporates data on each parcel's location and usage (e.g., designation as an apartment complex, an office building, a single-family residential building, etc.). Depending on its usage, each parcel may correspond to either a single building or a group of buildings. In total, there are 136,655 parcels in the area covered.

The testbed also links each parcel to its Traffic Analysis Zone (TAZ), i.e., link (d) in Figure 1. Traffic analysis zones are commonly used in traffic planning as a suitable way to divide the city into geographically smaller regions. The testbed's

³The area covered is between latitude 35.894145 longitude -80.198958 (N $35^{\circ}53'38.922''$, W $80^{\circ}11'56.284''$) and latitude 36.410277 longitude -79.157255 (N $36^{\circ}24'36.9972''$, W $79^{\circ}9'26.118''$)

⁴<https://www.nconemap.gov/pages/parcels>

TABLE II

ESTIMATED NUMBER OF VEHICLES FOR SELECTED PARCEL CATEGORIES

Category	Subcategory	Vehicle Estimate	Comment
APART	07-APT<5 UNITS	4	Apartments with less than 5 units
RESIDENTIAL	07-APT<5 UNITS	4	Multi-family houses with less than five units
GOV OWNED	07-APT<5 UNITS	4	Apartments with less than 5 units
APART	041-TOWNHOME	4	Only 1 in Guilford, has 4 units
COMM	07-APT<5 UNITS	4	Apartments with less than 5 units
COMM	09-TWNHSEAPT	4	Only 1 in Guilford, has 4 units
RESIDENTIAL	08-DUPLEX/TRIPLEX	3	Duplexes and Triplexes (chose 3 to be conservative)
MULTI-FAMILY<4	01-SFR	3	Multi-family houses with less than four units
MULTI-FAMILY<4	08-DUPLEX/TRIPLEX	3	Duplexes and Triplexes (chose 3 to be conservative)
GOV OWNED	08-DUPLEX/TRIPLEX	3	Duplexes and Triplexes (chose 3 to be conservative)
MULTI-FAMILY<4	07-APT<5 UNITS	3	Multi-Family Homes
MULTI-FAMILY<4	0	3	Multi-family residences with less than 4 units
OFFICE	08-DUPLEX/TRIPLEX	3	Duplexes and Triplexes (chose 3 to be conservative)
COMM	08-DUPLEX/TRIPLEX	3	Duplexes and Triplexes (chose 3 to be conservative)
APART	08-DUPLEX/TRIPLEX	3	Duplexes and Triplexes (chose 3 to be conservative)
IND	08-DUPLEX/TRIPLEX	3	Duplexes and Triplexes (chose 3 to be conservative)
RESIDENTIAL	01-SFR	1	SFR = Single Family Residential
CONDO	04-CONDO	1	Residential Condos (each condo has a separate parcel)
TOWNHOUSE	041-TOWNHOME	1	Townhomes
RESIDENTIAL	09-TWNHSEAPT	1	Townhouse
AGRI/HORT	01-SFR	1	Houses with Farmland
RESIDENTIAL	02-MANUFHM	1	Houses (manufactured houses)
COMM	01-SFR	1	Single Family Residence, near commercial district
GOV OWNED	01-SFR	1	Single Family Residences
DEVEL. RESTRICT.	01-SFR	1	Single Family Residences
IND	01-SFR	1	Single Family Residences
INSTITUTIONAL	01-SFR	1	Single Family Residences
SINGLE WIDE MH	0	1	Motorhomes
ASSIST LIV/SKILLCARE	01-SFR	1	Single Family Residences
OFFICE	01-SFR	1	Single Family Residences
APART	01-SFR	1	Single Family Residences
AIRPORT	01-SFR	1	Single Family Residences
VACANT	01-SFR	1	Single Family Residences
MFG HOM	02-MANUFHM	1	Manufactured Homes
TOWNHOUSE	04-CONDO	1	1 Condo per parcel
SCHOOL/COLL/UNIV	01-SFR	1	Single Family Residences
RESIDENTIAL	05-PATIOHM	1	Single Family Patio Homes
TWINHOME	012-TWIN HOME	1	Twin Homes
COMM	02-MANUFHM	1	Manufactured Homes
INSTITUTIONAL	02-MANUFHM	1	Manufactured Homes
LEASED	01-SFR	1	Single Family Residences
IND	02-MANUFHM	1	Manufactured Homes

traffic analysis zones were imported from open data provided by the U.S. Census Bureau.⁵ All the TAZs in the area we are studying are shown in Figure 5.

We estimate the number of vehicles for each parcel based on the parcel's usage specification as shown in Table II. A manual estimate with visual support from Google Maps and Google Streetview was performed for parcels that do not fall into any of the categories mentioned in Table II. The web interface for manual counting is also provided with the testbed in the file `scripts/manualvehiclecount.php`. The combination of vehicle estimation by category and manual counting creates the link labeled (c) in Figure 1 with respect to the total number of vehicles (both electric and conventional). Note that the vehicle estimates consider one vehicle per household in accordance with an evacuation scenario. For more realistic day-to-day usage scenarios, the numbers should be increased appropriately. The testbed easily accommodates such parameter modifications via updating the estimate for each category in the database and scaling the manual vehicle count in an appropriate manner. Since many of the parcels with a large number of manually counted vehicles are apartment complexes, upscaling counts by an appropriate factor would be sufficient for this class of parcels.

D. Prediction on Electric Vehicle Adoption

To predict the number of electric vehicles, we consider three main cases: one *base* case and two cases with higher EV penetration rates, which we denote as the *medium* and *high* cases. The base case directly uses historical data along with a prediction of future sales that is based on past electric vehicle sales backdated by the average vehicle age. This prediction is

TABLE III

NUMBER OF VEHICLES IN EACH TAZ

No.	TAZ	No. vehicles	No.	TAZ	No. vehicles
1	10100001	678	54	12804001	1583
2	10200001	1781	55	12805001	836
3	10300001	973	56	15100001	891
4	10401001	781	57	15300002	918
5	10403001	796	58	15300004	831
6	10404001	1087	59	15300006	295
7	10500001	1164	60	15401001	1474
8	10601001	1463	61	15402005	2686
9	10602001	2645	62	15500001	2567
10	10701001	1131	63	15600006	3865
11	10702001	1192	64	15703001	2622
12	10800001	1281	65	15704001	2455
13	10900001	993	66	15705001	948
14	11000001	813	67	15705002	438
15	11101001	2148	68	15706001	2455
16	11102001	1309	69	15707001	2566
17	11200001	2051	70	15800004	3072
18	11300001	1374	71	16003002	1726
19	11400001	1264	72	16005001	780
20	11500001	1294	73	16006001	488
21	11601001	1076	74	16006002	629
22	11602001	993	75	16007001	1073
23	11904001	2024	76	16007002	998
24	11905001	1843	77	16009001	916
25	12503001	1871	78	16009002	567
26	12504001	1103	79	16010001	1218
27	12505001	752	80	16011001	2162
28	12505002	1161	81	16101001	1150
29	12508001	1668	82	16101002	482
30	12509001	1088	83	16102001	1336
31	12510001	1438	84	16103001	1954
32	12511001	1378	85	16306001	2522
33	12511002	708	86	16405001	10
34	12601001	1816	87	16405002	923
35	12601002	972	88	16405003	34
36	12604001	1961	89	16406001	1632
37	12607001	995	90	16407001	1835
38	12608001	1241	91	16408001	803
39	12609001	2473	92	16409001	362
40	12609002	941	93	16409002	626
41	12610001	1133	94	16502001	2365
42	12611001	1140	95	16503001	913
43	12612001	2618	96	16503002	1223
44	12617001	971	97	16505001	1621
45	12703001	1921	98	16506001	488
46	12704001	1310	99	16506002	1363
47	12705001	1444	100	16702006	2346
48	12706001	1429	101	16800001	814
49	12707001	1132	102	17100003	541
50	12803001	469	103	17100004	599
51	12803002	865	104	17200003	654
52	12803003	1478	105	17200004	393
53	12803004	437	106	98010001	2931

likely to be a conservative estimate since it does not incorporate increasing electric vehicle adoption rates. The medium and high cases are based on projections from USDRIVE [1] that account for increasing interest in buying electric vehicles. Figures 6–8 show the percentages of electric vehicles in each TAZ for each case (base, medium, and high). Additionally, to perform a sensitivity analysis on power grid impacts, we consider an *extreme* case in one of the demonstrations in Section IV. This extreme case is the same as the *high* case but with additional EVs assigned at random to reach an 80% EV penetration rate.

1) *Base Case*: To generate a reasonable distribution of their current status, we used electric vehicle registration data from

⁵<https://www2.census.gov/geo/tiger/TIGER2010/TAZ/2010/>

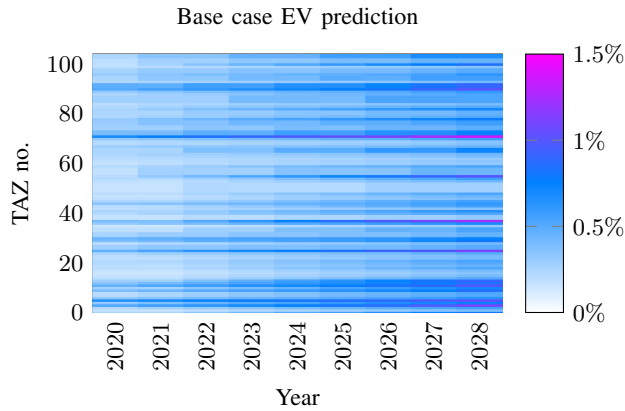


Fig. 6. Percentage of electric vehicles in each TAZ in the base case prediction.

Guilford County in 2019.⁶ Electric vehicles were then distributed among the census tracts proportionally to the number of households and the median income in each census tract. In this way, census tracts with more households and higher incomes are assigned higher fractions of electric vehicles.

For the base case, we used data on the average vehicle age based on household income from the National Household Travel Survey.⁷ The data are extrapolated to the year 2028. This extrapolation is then combined with the mean household income in each census tract⁸ to find the average vehicle age for each census tract between the year 2020 and the year 2028. We assume here that the mean household income will not change significantly during the prediction period.

Once we know the expected average age of vehicles in each census tract, the number of new electric vehicles added yearly to each census tract is estimated by the fraction of electric vehicles that were sold the average-vehicle-age ago. For example, if the average vehicle age is 10 years, we use vehicle sales from 2015 to predict how many new EVs will appear in the year 2025. This approach captures the fact that census tracts with newer vehicles, on average, are more likely to consider buying electric vehicles.

To find the historical market penetration rate, we divided the number of EVs sold in the US each year⁹ by the total vehicle sales for the same year.¹⁰ To adapt those fractions to Guilford county, we utilized data from 2019 on the number of registrations of electric vehicles in North Carolina¹¹ and the total number of electric vehicles sold in Guilford county.¹²

Since TAZs are more granular than census tracts, the number of electric vehicles were split equally among the census tracts when there are several TAZs within a census tract. For

⁶<https://www.ncdot.gov/initiatives-policies/environmental/climate-change/Pages/zev-registration-data.aspx>

⁷<https://nhts.ornl.gov>

⁸<https://data.census.gov/cedsci/table?q=income&g=0500000US37081.140000&tid=ACSS5Y2018.S1901&moe=false&hidePreview=true>

⁹See <https://electricdrive.org/index.php?ht=d/sp/i/20952/pid/20952>, <https://insideevs.com/news/344006/monthly-plug-in-report-card-archive/>, and <https://afdc.energy.gov/data/10567>

¹⁰<https://fred.stlouisfed.org/series/TOTALSA#0>

¹¹<https://afdc.energy.gov/data/10962>

¹²<https://www.ncdot.gov/initiatives-policies/environmental/climate-change/Pages/zev-registration-data.aspx>

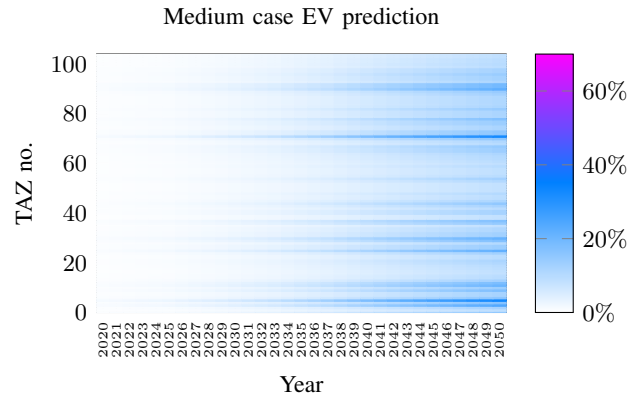


Fig. 7. Percentage of electric vehicles in each TAZ in the medium case prediction.

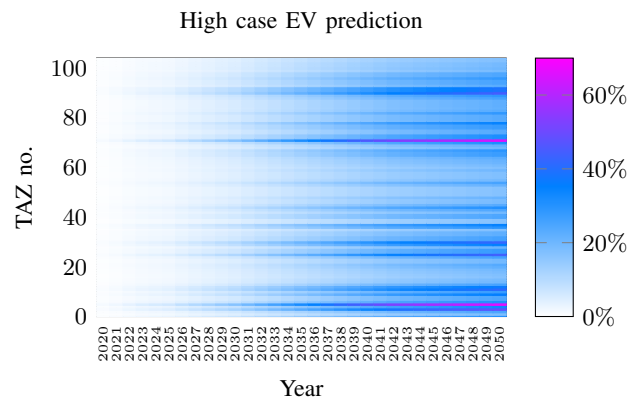


Fig. 8. Percentage of electric vehicles in each TAZ in the high case prediction.

a few census tracts, parts of the tracts were located outside the area covered. In this case, the prediction of the number of electric vehicles was scaled down in proportion to the land area within the TAZ.

To get the percentage of electric vehicles within each TAZ, we adopted the projected total fleet size (including both electric and conventional vehicles) for the United States from 2020–2050¹³ to Guilford county by utilizing the percentage of the total number of vehicles sold in Guilford county¹⁴ for 2019. By assuming that that Guilford county accounts for a constant proportion of all vehicles in the United States, we then projected values for the total number of vehicles in Guilford from 2020 to 2050. This total fleet size was split in proportion to the number of households in each census tract. The total fleet sizes were adjusted to TAZs in the same manner as the EVs, finally enabling calculation of the percentage of electric vehicles in each TAZ.

2) *Medium and High Cases:* Predictions from US-DRIVE [1] were used to construct the medium and high cases. Historical data of the electric vehicle sales per state¹⁵ and per county in North Carolina¹⁶ were used to apply the USDRIVE

¹³<https://www.eia.gov/outlooks/aeo/data/browser/#/>

¹⁴<https://www.ncdot.gov/initiatives-policies/environmental/climate-change/Pages/zev-registration-data.aspx>

¹⁵<https://afdc.energy.gov/data/10962>

¹⁶<https://www.ncdot.gov/initiatives-policies/environmental/climate-change/Pages/zev-registration-data.aspx>

predictions to Guilford county. To spatially distribute the predicted number of electric vehicles in each census tract, we assumed that the electric vehicles will be distributed proportionally to both the current number of households in each census tract and the median household income in each census tract. The predicted numbers of electric vehicles for each census tract were then converted to predicted numbers of electric vehicles for each TAZ by following the same methodology as for the base case scenario. The same methodology as for the base case was also used to convert the absolute number of electric vehicles to the fraction of electric vehicles.

Note that we only use these predictions of vehicle electrification trends to determine the *fraction* of electric vehicles in each TAZ. In the testbed, the total number of vehicles remains constant every year since the testbed does not include further housing or other infrastructure development, such as the expansion of the power grid. In this way, we maintain consistency between the capacities of the electric and transportation infrastructure and the vehicle travel and charging demands, thus avoiding the need to consider infrastructure expansion over time.

Interpreting the fraction of electric vehicles within a TAZ as the probability that each vehicle associated with a parcel is electric, the last part of the link (c) in Figure 1 is completed, and hence all data needed to perform simulations in the testbed are in place. In the next section, we will describe the pipeline for running simulations in the testbed.

III. TESTBED USAGE

The testbed consists of several modules that can be run either jointly or separately, given that the data each module depends on has been generated at some earlier time. The testbed is applied to analyze *scenarios*, each of which has the following properties:

- *Fraction of electric vehicles*: A scenario can either have a fixed fraction of electric vehicles, i.e., every vehicle has a fixed probability of being electric, or a prediction using the approach described in the previous section.
- *Departure time*: Each vehicle departs at a specified time.
- *Charging schedule*: Each electric vehicle starts and stops charging at specified times, using a constant charging rate.

The evacuations that we consider as illustrative applications for the testbed additionally require specifying:

- The TAZs that will be evacuated.
- The safe node for the evacuation, i.e., where the vehicles should go once they depart. Since the traffic simulation only covers the area surrounding Greensboro, this safe node corresponds to a point on a freeway at the perimeter of the city, as is typically the case in evacuation planning problems [6], [7].

A. Data Pre-processing Pipeline

To facilitate the usage of this testbed methodology for other regions, the pre-processing scripts we developed for Greensboro are included in the testbed. After obtaining the SUMO network, OpenDSS network, and parcel data, the pipeline for linking the different datasets can be done with

the code `scripts/data_preprocessing.py`. The pre-processing script creates a common ground through an SQLite database that both the traffic simulator SUMO and the power simulator OpenDSS draw upon while providing relative independence in terms of running different kinds of simulations, as they both read from the database while not interfering with each other. While most aspects of this pre-processing are straightforward to extend to different regions, note that the data will still likely require some manual processing, such as adding vehicle estimates for some categories of parcels, fixing broken roads in the imported SUMO network, etc.

For the scenarios we demonstrate in this paper, note that all of the pre-processing is already done, and the outcome is stored in the database that comes with the testbed.

B. Overview of the Workflow

Once the preprocessing is done, the testbed is executed using the Python script `interactive_simulator.py`. Before running this script, the parameters listed in Table IV need to be specified. The script then displays a menu in the terminal where the user can choose which stages of the workflow the user wants to (re)-run. The different stages are described below:

1) *Copying Files*: The testbed first copies configuration files for the SUMO and OpenDSS simulators onto the specified file path for the current scenario. These configuration files are not scenario dependent, but the user may want to change some of the simulator-specific parameters in these files. Some parameters for the SUMO simulator, such as maximum simulation time, can be changed directly in the generated configuration file for the simulator.

Each scenario will have a copy of the simulation files for the SUMO configuration, power grid data, traffic flow files, vehicle route files, etc. For example, two simulations of the same region with the same simulated vehicle locations but different electric vehicle penetration rates or evacuation routes will share the same database but have separate working directories and generate result files in different sub-directories.

The SUMO simulator requires a detailed description of each vehicle's path in the traffic network. To obtain such a low-level description, the SUMO tool `duarouter`¹⁷ is utilized.

2) *Traffic Simulation Configuration*: In this stage, various configurations for the SUMO simulator are generated. First, the vehicle generation step populates the database with vehicles for the scenario and also determines whether each vehicle is electric or conventional. Next, the testbed assigns departure and charging times for each vehicle in the specified scenario. Both of these steps utilize random numbers, so rerunning the testbed with the same scenario may result in updates to these properties for each vehicle. All other steps in the workflow are deterministic and will hence yield the same results if they are rerun.

3) *Run Simulations*: The next stage runs the SUMO simulator and the OpenDSS simulator with the parameters set in the main script using the previously created configuration files. Each simulator produces separate output files that can be

¹⁷<https://sumo.dlr.de/docs/duarouter.html>

TABLE IV
PARAMETERS TO BE SET IN MAIN SIMULATOR SCRIPT

Parameter	Description
scenario_name	A unique name for each scenario
working_dir	The location where the output files will be stored
ev_penetration_rate	A value between 0 and 1 if the scenario has a fixed penetration rate, -1 if using any of the predicted rates
year_prediction	The year considered when utilizing the “base”, “medium”, or “high” cases
prediction_level	Either “base”, “medium”, or “high” when utilizing one of these cases
load_per_charging_ev	The electric power demand from each electric vehicle when charging
charging_time	The amount of time before departure that each vehicle should start charging
departure_window	The window during which each vehicle will randomly depart
tazs_to_evacuate	Evacuation specific parameter: Set of TAZs to be evacuated
evac_edge	Evacuation specific parameter: The SUMO edge all vehicles head towards

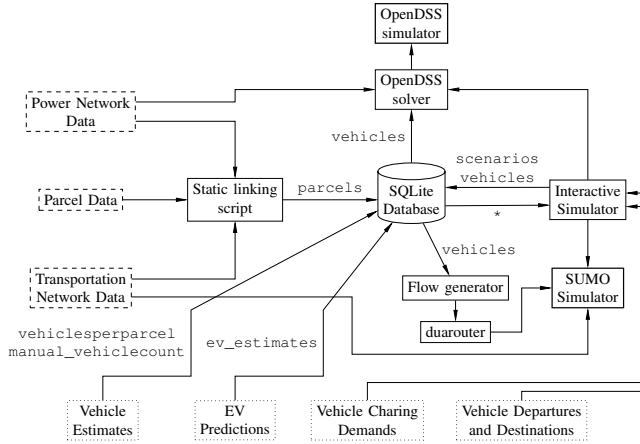


Fig. 9. The detailed architecture of the testbed. The dashed boxes are data obtained from exogenous data sources, while the dotted boxes represent data provided by the user. Next to some of the arrows, the figure indicates which table in the database is used or changed by a script. The simulator utilizes several of the generated tables when creating scenarios with vehicles. These dependencies are denoted an asterisk.

analyzed. Several scripts for analyzing the simulators’ outputs are included with the testbed, such as the scripts for generating the plots in the demonstration cases shown in the next section.

C. Architecture

Figure 9 describes the testbed’s architecture. The figure shows when different tables are created or expanded and which component uses each table. Note that the vehicle table contains the vehicles for every scenario, but only the vehicles for the specific scenario are selected by the simulator.

IV. DEMONSTRATIONS OF THE TESTBED

This section first presents an illustrative application of the testbed via two evacuation scenarios (a small scenario that runs for a few minutes on a personal computer and a large scenario which requires several hours to run the traffic simulator), followed by a discussion of other potential applications.

For both evacuation scenarios, the vehicles evacuate to Route 40 east of Greensboro, and each vehicle will be routed such as it will take its shortest path with respect to travel time as if there were no other vehicles present. For the small scenario, we are using the EV prediction rates for the year 2040, while for the large scenario, we are using the EV prediction rates for the year 2045.

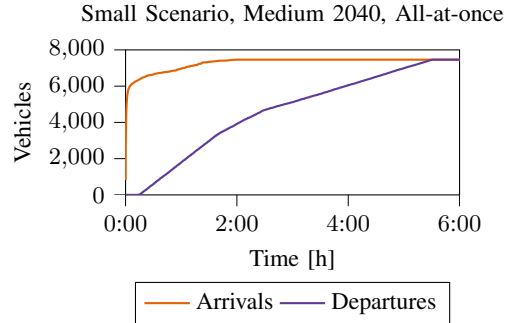


Fig. 10. Cumulative departure and arrival curves for the Small Scenario Medium 2040 All-at-once.

A. Small Evacuation Scenario

As a simple demonstration scenario that can run quickly on a personal computer, the testbed comes with a scenario where only a small part of the region covered by the testbed is evacuated. The region consists of six TAZs, outlined in green in Figure 5. We run several variants of this scenario, considering either the simultaneous departures of all vehicles or vehicle departure times that are spread out randomly over a two-hour window. The scenarios are also run with different penetration rates of electric vehicles to illustrate the evacuation’s impacts on the power grid.

Table V shows the total number of vehicles and the number of electric vehicles for each scenario. Moreover, the performance of the transportation network is shown. From the performance metrics, we can see that it takes approximately the same time to evacuate regardless if the vehicles are spread out over a two-hour window or not, with the vehicles spending less time waiting in the transportation network when their departure time is spread out. This can further be seen in Figures 10 and 11, where we plot the cumulative number of departures and arrivals. In both figures, the curves intersect at almost the same point, but the area between the curves is considerably less for the two-hour departure window scenario, meaning that the vehicles spend less time on the road.

To study the performance of the power grid, we will use the number of overloaded power grid components and the severity of these overloads to compare different evacuation charging schedules. A component is considered overloaded if the current flowing through it is above its specified normal current flow limit. Figures 12 and 13 demonstrate how the penetration rate of EVs and the timing of their charging can

TABLE V
STATISTICS REGARDING THE TRANSPORTATION NETWORK FOR THE SMALL SCENARIO

	Medium 2040 All-at-once	Medium 2040 2 hours	High 2040 All-at-once	High 2040 2 hours
Number of vehicles	7461	7461	7461	7461
Number of EVs	621	621	1552	1552
Departure window	0 h	2 h	0 h	2 h
Total time to evacuate [s]	19816	19920		
Average speed [m/s]	5.32	10.58		
Average duration [s]	7712.58	4851.47	Same as Medium 2040 All-at-once	Same as Medium 2040 2 hours
Average waiting time [s]	4789.48	2397.17		
Average time loss [s]	6868.27	4007.48		
Average departure delay [s]	543.12	2.79		

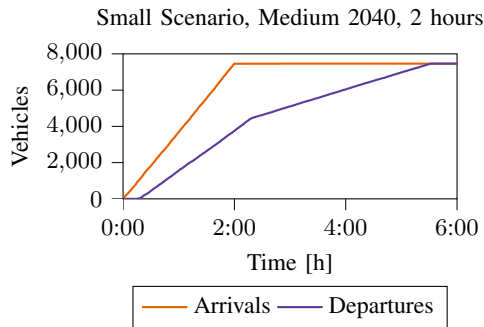


Fig. 11. Cumulative departure and arrival curves for the Small Scenario Medium 2040 with a two-hour departure window.

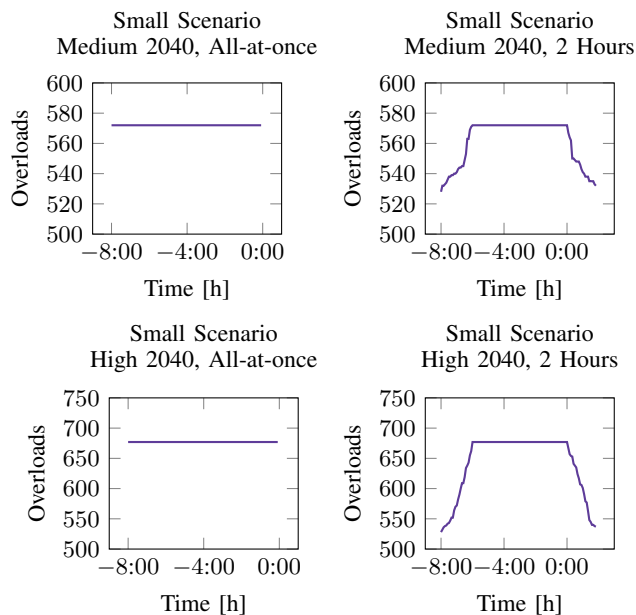


Fig. 12. Overloads per interval for medium and high EV penetration rates in the Small Scenario. In the left column, all the electric vehicles charge simultaneously. In the right column, the vehicle charging start times are randomly assigned over a two-hour window.

impact the number and severity of overloads, respectively. The left-hand figures depict the scenarios where all EVs charge simultaneously for eight hours, while the right-hand figures represent scenarios where the charging start times of all EVs are randomly assigned over a two-hour window. Figure 12 shows that while simultaneous charging of all EVs reduces the overall charging time, this also results in more overloads over a longer period of time. In addition, the figures on the top and bottom illustrate that a higher

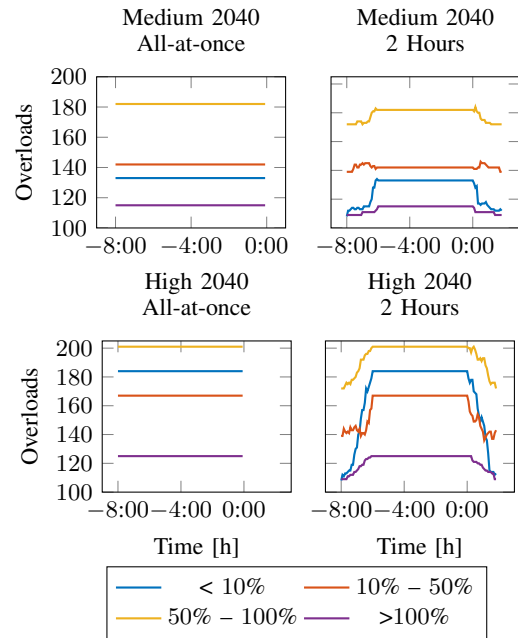


Fig. 13. Overloads under 10% (blue), between 10% and 50% (orange), between 50% and 100% (yellow), and over 100% (purple) for medium and high EV penetration rates in the small scenario. In the left column, all electric vehicles charge simultaneously. In the right column, the vehicle charging start times are randomly assigned over a two-hour window.

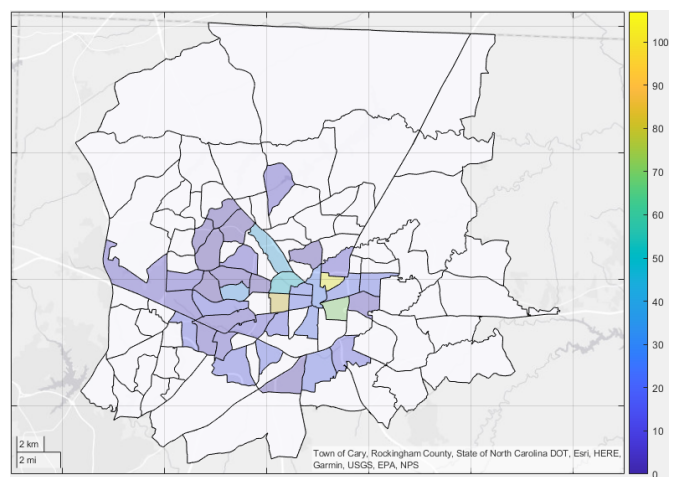


Fig. 14. Map showing the distribution of the power grid overloads by TAZ during the last charging interval of the EVs in the scenario High 2040, All-at-once. White TAZs have no overloads in them, while the color gradient indicates the number of overloaded components in all other TAZs.

number of EVs (High EV Penetration) can result in more overloads of power grid components than a moderate number of EVs (Medium EV Penetration). Furthermore, Figure 13 demonstrates how overloads of all severities increase the more EVs charge simultaneously. Overloads under 10% see the highest increase, followed by overloads between 10% and 50%, overloads between 50% and 100%, and overloads over 100%, respectively. These overloads are distributed across different levels and locations of the distribution network and the TAZs. Figure 14 shows a map of all TAZs and the number of power grid overloads occurring in each when all EVs are charging simultaneously in the High 2040 scenario. While many TAZs see a small number of overloads, most overloads are concentrated in the few TAZs which are evacuated in this scenario. To summarize, this small scenario shows that spreading out the departure of the vehicles reduces the duration of power grid overloads, while the total time to evacuate remains nearly the same (0.52% increase).

B. Large Evacuation Scenario

For the large evacuation scenario, we consider all the TAZs displayed in Figure 3. We assign a random departure time for each vehicle within an eight-hour window. A summary of the number of vehicles considered and the performance of the transportation network is given in Table VI. As can be seen in Figure 3, the power network only covers part of the area, which means that only half of the total number of EVs will be included in the power grid simulator. We emphasize, however, that all TAZs are included in the traffic simulator.

Similar to the small scenario, the cumulative departure and arrival rate is shown in Figure 15. This large scenario demonstrates the need to develop optimized evacuation plans since a naive routing where each vehicle is taking its shortest path with respect to uncongested does not seem to be a particularly efficient strategy. As can be seen in Table VI, the vehicles spend a lot of time waiting in the traffic network, and it is reasonable to believe that a more efficient routing strategy could alleviate part of this waiting time by making some vehicles take longer but less congested routes.

For the power grid simulations in the large scenario, we consider medium, high, and extreme EV penetration cases. Figure 16 shows the number of overloaded components throughout the charging period. As expected, the number of overloaded components increases considerably as we increase the number of EVs in the system, with the extreme case having 1406% and 401% more overloads than the medium and high cases, respectively. The distribution of these overloads' severity is illustrated in Figure 17. For all three penetration rates, overloads in the range of 10% to 50% account for the most of any category in this figure.

In contrast to the small scenario, where charging a relatively small number of electric vehicles had almost no impact on the number of voltage violations, the large scenario showed a significant increase in undervoltage violations across all three cases. This is evident in Figure 18, which shows the number of undervoltage violations peaking at 5604, 151514, and 154118 for the medium, high, and extreme cases, respectively. It

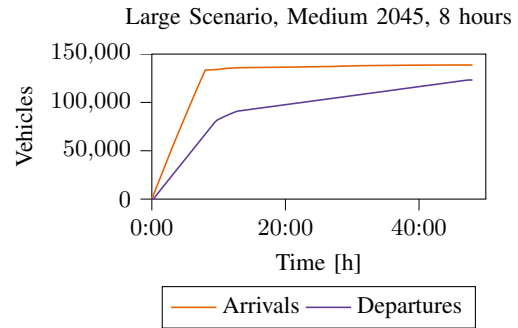


Fig. 15. Cumulative departure and arrival curves for the large scenario where the vehicles depart during an eight-hour window.

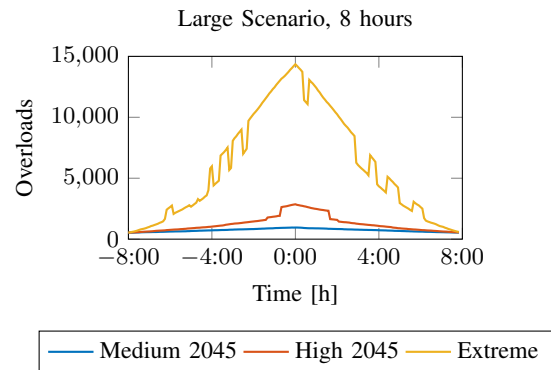


Fig. 16. Overloads per interval for Medium 2045, High 2045, and Extreme EV penetration rates in the large scenario. Vehicle charging start times are randomly assigned over an eight-hour window.

is worth noting that Figures 16–18 exhibit several discrete “drops” and “jumps” caused by the OpenDSS simulator’s discrete controllers’ efforts to minimize violations in the system. Figure 19 depicts the reduction in undervoltages and overloaded components with and without these control efforts. These discrete changes in the system, especially transformer tap changes, help to reduce overloads and greatly decrease the number of voltage violations.

C. Other Potential Applications

While the current setup of the testbed is configured for evacuation scenarios, the testbed can easily be adapted to normal operational scenarios as well. For instance, one could compare weekday versus weekend transit behaviors by using parcel and zoning information to configure vehicles in the testbed to transit from homes to workplaces, schools, and commercial centers. The testbed could also be useful for studying the impacts of vehicle fleets (school buses, delivery vehicles, etc.) with different charging schedules.

To configure such scenarios, one would adjust the vehicle estimates for the parcel categories to make them match the scenario. Also, the flow and generation parts in the testbed workflow would need to be changed, as they are currently designed to route all the vehicles to one destination. For this, SUMO tools like activitygen¹⁸ would be valuable.

¹⁸<https://sumo.dlr.de/docs/activitygen.html>

TABLE VI
STATICS ABOUT THE TRANSPORTATION NETWORK FOR THE LARGE SCENARIO

	Medium 2045 8 hours	High 2045 8 hours
Number of vehicles	141046	141046
Number of EVs	13201	29743
of which connected to the power grid	7403	16712
Departure window	8 h	8h
Total time to evacuate	> 48 h	
Average speed [m/s]	7.72	
Average duration [s]	27169.80	Same as Medium
Average waiting time [s]	27169.80	2045 8 hours
Average time loss [s]	26353.44	
Average departure delay [s]	1922.22	

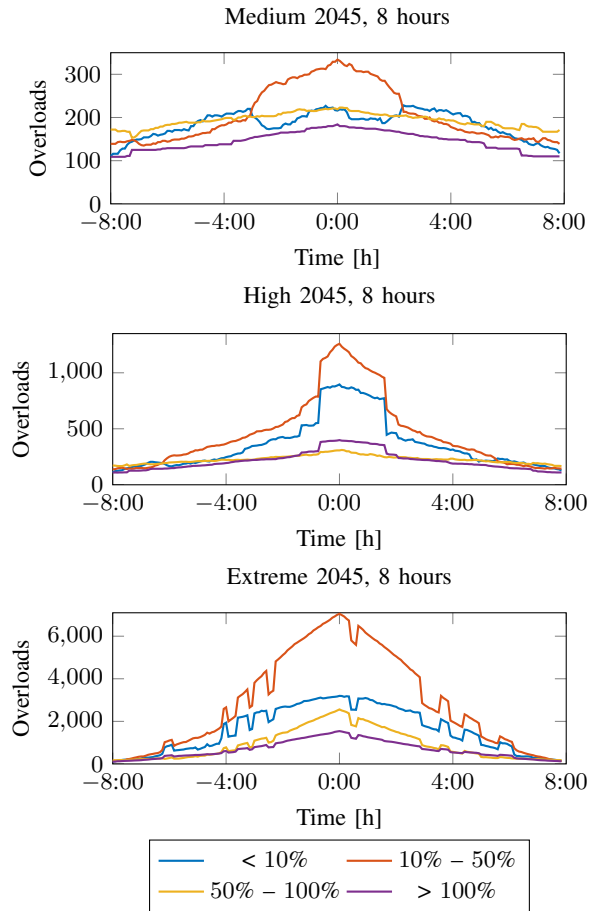


Fig. 17. Overloads under 10% (blue), between 10% and 50% (orange), between 50% and 100% (yellow), and over 100% (purple) for medium, high, and extreme EV penetration rates in the large scenario. Vehicle charging start times are randomly assigned over an eight-hour window.

V. CONCLUSION AND FUTURE WORK

In this work, we have presented a testbed that jointly simulates a transportation network and the power grid in the presence of electric vehicles that need to charge before departure. The testbed is constructed by linking together publicly available data from different sources, such as road map data from OpenStreetMap, parcel data from the State of North Carolina, and power grid data from the SMART-DS dataset. The open-source simulators SUMO and OpenDSS are then utilized by the testbed to simulate the transportation network and the power grid. To demonstrate how the testbed can be utilized, we performed simulations of both small- and large-

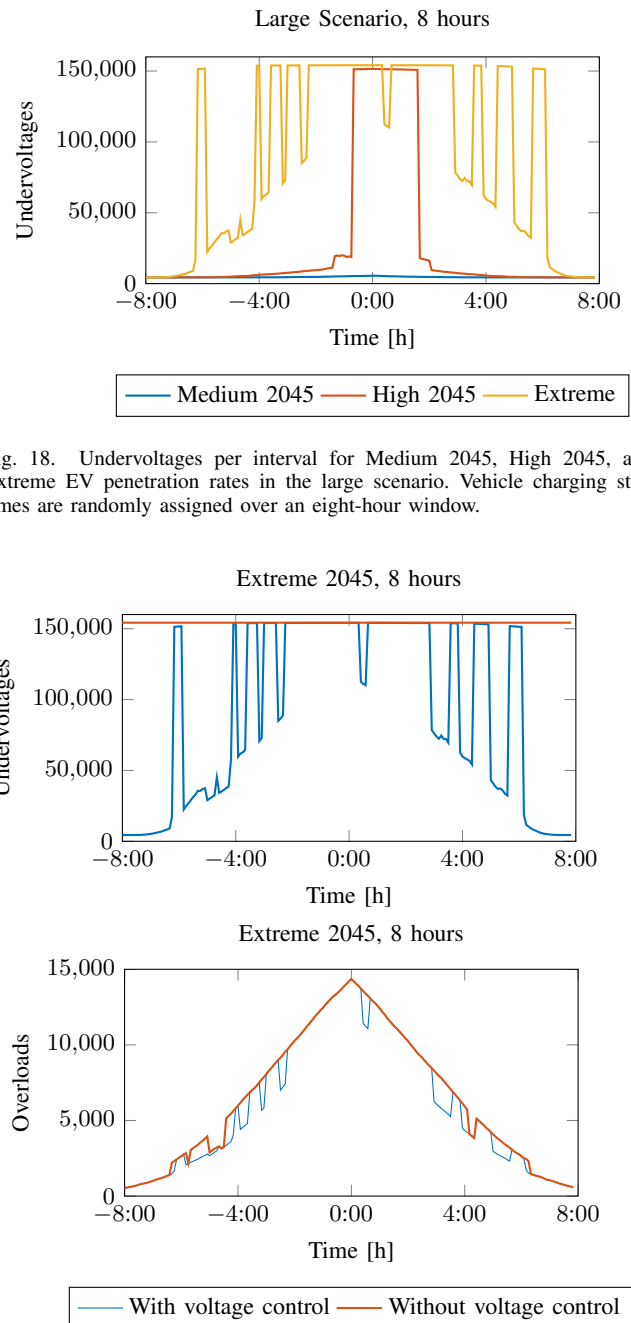


Fig. 18. Undervoltages per interval for Medium 2045, High 2045, and Extreme EV penetration rates in the large scenario. Vehicle charging start times are randomly assigned over an eight-hour window.

Fig. 19. Comparison of undervoltages (left) and overloads (right) with and without allowing voltage control efforts in OpenDSS. Results where tap changes, voltage regulation, and capacitor switchings are allowed are shown in blue. Results where these control efforts are turned off are shown in orange.

scale evacuation scenarios. The simulations show the need to optimize evacuation scenarios while also demonstrating that synergies can be achieved by considering both systems jointly. Spreading out the vehicles' departure times may only cause small increases in the total evacuation time after the vehicles depart while substantially reducing the number and severity of overloaded power grid components.

Using the testbed presented in this paper, our ongoing work is continuing to analyze and optimize evacuation scenarios. Our ultimate goal is to optimally schedule vehicle charging as well as departure times and routes while jointly considering the capabilities of both the power grid and the transportation system. To this end, we envision extensions and enhancements of the testbed, such as modeling cascading failures in the electric grid model. Sufficiently large overloads of distribution lines and transformers may cause protection systems like fuses and breakers to operate, disconnecting the overloaded components, de-energizing portions of the grid, and potentially overloading other components. Modeling the behavior of protection systems would thus better represent possible outages during both normal and extreme operating conditions. Additionally, we aim to couple the vehicle energy consumption used for particular trips between SUMO and OpenDSS. For the evacuation scenarios that are the focus of the existing testbed, it suffices to fully charge the vehicles prior to departure. Conversely, trips during normal operating conditions may not require fully charging all vehicles prior to departure. Capturing this behavior would thus improve modeling accuracy during normal operating conditions.

ACKNOWLEDGEMENTS

The authors would like to thank Yilun Chen for his support with the development and documentation of the testbed, Katelyn Iles for her help with obtaining vehicle estimates, Ravi Kodali for his support with power grid visualizations and running OpenDSS simulations, and Samuel Talkington for assisting with testing the tools in the testbed.

REFERENCES

- [1] US Drive, "Summary report on EVs at scale and the US electric power system," 2019. <https://www.energy.gov/sites/prod/files/2019/12/f69/GITT%20ISATT%20EVs%20at%20Scale%20Grid%20Summary%20Report%20FINAL%20Nov2019.pdf>.
- [2] L. Calearo, A. Thingvad, K. Suzuki, and M. Marinelli, "Grid loading due to EV charging profiles based on pseudo-real driving pattern and user behavior," *IEEE Transactions on Transportation Electrification*, vol. 5, no. 3, pp. 683–694, 2019.
- [3] Y. Yu, D. Reihns, S. Wagh, A. Shekhar, D. Stahleder, G. R. C. Mouli, F. Lehfuss, and P. Bauer, "Data-driven study of low voltage distribution grid behaviour with increasing electric vehicle penetration," *IEEE Access*, vol. 10, pp. 6053–6070, 2022.
- [4] S. Rahman, I. A. Khan, A. A. Khan, A. Mallik, and M. F. Nadeem, "Comprehensive review & impact analysis of integrating projected electric vehicle charging load to the existing low voltage distribution system," *Renewable and Sustainable Energy Reviews*, vol. 153, p. 111756, 2022.
- [5] G. Nilsson and S. Coogan, "A compartmental dynamical network flow model for evacuation planning of cities," in *IEEE Conference on Control Technology and Applications (CCTA)*, pp. 1005–1010, 2022.
- [6] M. H. Hasan and P. Van Hentenryck, "Large-scale zone-based evacuation planning, Part I: Models and algorithms," *Networks*, 2020.
- [7] M. H. Hasan and P. Van Hentenryck, "Large-scale zone-based evacuation planning, Part II: Macroscopic and microscopic evaluations," *Networks*, 2020.
- [8] K. Feng, N. Lin, S. Xian, and M. V. Chester, "Can we evacuate from hurricanes with electric vehicles?," *Transportation Research Part D: Transport and Environment*, vol. 86, p. 102458, 2020.
- [9] S. A. Adderly, D. Manukian, T. D. Sullivan, and M. Son, "Electric vehicles and natural disaster policy implications," *Energy Policy*, vol. 112, pp. 437–448, 2018.
- [10] C. D. MacDonald, L. Kattan, and D. Layzell, "Modelling electric vehicle charging network capacity and performance during short-notice evacuations," *International Journal of Disaster Risk Reduction*, vol. 56, p. 102093, 2021.
- [11] P. A. Lopez, M. Behrisch, L. Bieker-Walz, J. Erdmann, Y.-P. Flötteröd, R. Hilbrich, L. Lücken, J. Rummel, P. Wagner, and E. Wießner, "Microscopic traffic simulation using SUMO," in *21st IEEE International Conference on Intelligent Transportation Systems*, 2018.
- [12] R. C. Dugan and T. E. McDermott, "An open source platform for collaborating on smart grid research," in *IEEE Power and Energy Society General Meeting*, 2011.
- [13] M. Rapelli, C. Casetti, and G. Gagliardi, "Vehicular traffic simulation in the city of Turin from raw data," *IEEE Transactions on Mobile Computing*, vol. 21, no. 12, pp. 4656–4666, 2022.
- [14] L. Codeca, R. Frank, S. Faye, and T. Engel, "Luxembourg SUMO Traffic (LuST) Scenario: Traffic demand evaluation," *IEEE Intelligent Transportation Systems Magazine*, vol. 9, no. 2, pp. 52–63, 2017.
- [15] F. B. Thiam and C. L. DeMarco, "Automated transmission expansion and routing incorporating electric and geographic criteria," in *IEEE Power Energy Society Innovative Smart Grid Technologies Conference (ISGT)*, 2016.
- [16] Z. Huang, R. Huang, Y. V. Makarov, S. J. Young, R. Fan, A. Tbaileh, Z. Hou, J. O'Brien, J. C. Fuller, J. Hansen, and L. D. Marinovici, "Sustainable data evolution technology (SDET) for power grid optimization (final report)," Tech. Rep. PNNL-28338, Pacific Northwest National Laboratory, December 2018. <https://www.osti.gov/biblio/1524091>.
- [17] F. Fioretto, T. W. K. Mak, and P. Van Hentenryck, "Differential privacy for power grid obfuscation," *IEEE Transactions on Smart Grid*, vol. 11, no. 2, pp. 1356–1366, 2020.
- [18] A. B. Birchfield, E. Schweitzer, M. H. Athari, T. Xu, T. J. Overybe, A. Scaglione, and Z. Wang, "A metric-based validation process to assess the realism of synthetic power grids," *Energies*, vol. 10, no. 8, p. 1233, 2017.
- [19] A. B. Birchfield, T. Xu, K. M. Gegner, K. S. Shetye, and T. J. Overybe, "Grid structural characteristics as validation criteria for synthetic networks," *IEEE Transactions on Power Systems*, vol. 32, no. 4, pp. 3258–3265, 2017.
- [20] B. Palmintier, T. Elgindy, C. Mateo, F. Postigo, T. Gómez, F. de Cuadra, and P. D. Martinez, "Experiences developing large-scale synthetic US-style distribution test systems," *Electric Power Systems Research*, vol. 190, p. 106665, 2021. Presented at the *21st Power Systems Computation Conference (PSCC 2020)*.
- [21] The National Renewable Energy Laboratory. (NERL), "SMART-DS: Synthetic models for advanced, realistic testing: Distribution systems and scenarios." <https://www.nrel.gov/grid/smart-ds.html>.
- [22] S. Xie, Z. Hu, J. Wang, and Y. Chen, "The optimal planning of smart multi-energy systems incorporating transportation, natural gas and active distribution networks," *Applied Energy*, vol. 269, p. 115006, 2020.
- [23] W. Gan, M. Shahidehpour, M. Yan, J. Guo, W. Yao, A. Paaso, L. Zhang, and J. Wen, "Coordinated planning of transportation and electric power networks with the proliferation of electric vehicles," *IEEE Transactions on Smart Grid*, vol. 11, no. 5, pp. 4005–4016, 2020.
- [24] K. Lai, T. Chen, and B. Natarajan, "Optimal scheduling of electric vehicles car-sharing service with multi-temporal and multi-task operation," *Energy*, vol. 204, p. 117929, 2020.
- [25] Y. Shuai, Y. Zhang, F. Liu, X. Qiao, Y. Xiong, and Y. Zeng, "Co-simulation of power grid, information network and transportation network simulation system," in *IEEE 2nd International Conference on Software Engineering and Artificial Intelligence (SEAI)*, pp. 199–203, 2022.
- [26] Y. Zheng, S. Niu, Y. Shang, Z. Shao, and L. Jian, "Integrating plug-in electric vehicles into power grids: A comprehensive review on power interaction mode, scheduling methodology and mathematical foundation," *Renewable and Sustainable Energy Reviews*, vol. 112, pp. 424–439, 2019.
- [27] W. Wei, D. WU, Q. WU, M. Shafie-Khah, and J. P. Catalão, "Interdependence between transportation system and power distribution system: A comprehensive review on models and applications," *Journal of Modern Power Systems and Clean Energy*, vol. 7, no. 3, pp. 433–448, 2019.
- [28] U.S Department of Energy, "Alternative fuels data center," 2023. https://afdc.energy.gov/fuels/electricity_infrastructure.html.